Acta Cryst. (1996). B52, 32–37

Structure of ζ-Phase Plutonium–Uranium

A. C. LAWSON,[a] J. A. GOLDSTONE,[a] B. CORT,[a] R. J. MARTINEZ,[a] F. A. VIGIL,[a] T. G. ZOCCO,[a] J. W. RICHARDSON JR[b] AND M. H. MUELLER[b]

[a]*Los Alamos National Laboratory, Los Alamos, NM 87545, USA, and* [b]*Intense Pulsed Neutron Source, Argonne National Laboratory, Argonne, IL 60439, USA*

(*Received 3 May 1995; accepted 22 May 1995*)

Abstract

The structure of the ζ-phase in the Pu–U system has been determined by neutron powder diffraction. The phase crystallizes in space group $R\bar{3}m$ with 58 atoms in the primitive unit cell and 10 atoms in the asymmetric unit. The structure is characterized by many short bonds and fits the general pattern of the light actinides. Thermal expansion and elastic data were obtained from the diffraction experiments.

1. Introduction

The crystal structures of metallic elements are usually simple. However, a number of metallic elements have structures of surprising complexity. These elements appear in regions of the periodic system that are characterized by electronic instability, such as the beginning of the 5*f* series and the middle of the 3*d* series. The normally stable structure of plutonium metal is monoclinic, with eight distinct atom types and 16 atoms in the unit cell (Zachariasen & Ellinger, 1963*b*). Similarly, α-Mn occurs in the middle of the 3*d* electronic series and has a complicated body-centered cubic structure with four atom types and 58 atoms per unit cell (Bradley & Thewlis, 1927). Details of these structures may be found in the monograph by Donohue (1974).

The reason for the occurrence of these complex structures is not known in detail, but it has been speculated for a long time that the structures are stabilized by the simultaneous presence of metal atoms with different valences or configurations (Bradley & Thewlis, 1927; Grigorvich, 1988) For example, α-Mn is isostructural with a number of intermetallic compounds known as χ-phases, which are typified by materials such as Ti_5Re_{24}; β-U is isostructural with the σ-phase commonly found in transition metal alloys; β-UH_3 is isostructural with the well known β-W structure, typified by Nb_3Sn, if one neglects the interstitial H atoms. Elements or compounds that gain stability by having the same element in more than one valence or configuration may be usefully referred to as self-intermetallic compounds. It is of the greatest interest to study the occurrence of such idiosyncratic structures in the periodic system. A better understanding of this phenomenon would benefit our knowledge of transition and actinide materials in particular, and our knowledge of the metallic bond in general.

The interactinide alloy systems show additional complex phases whose structures are for the most part unknown. One of these alloy structures is the ζ-phase in the Pu–U system. The phase diagram is shown in Fig. 1 (Ellinger, Elliott & Cramer, 1959). This diagram has been generally confirmed in a recent study (Okamoto, Maeda, Suzuki & Ohmichi, 1994). Ellinger *et al.* (Ellinger, Elliott & Cramer, 1959) studied the X-ray diffraction of the intermediate phases in the Pu–U system. They indexed the observed reflections in the ζ-phase on the basis of a primitive cubic cell, with a lattice constant in the range 10.692–10.651 Å, depending on composition (35–70% U). However, they also observed some deviation from cubic symmetry, especially at high temperatures. From the measured density of the ζ-phase, they found an atomic density of 58 atoms per unit cell. Ellinger *et al.* also reported *d*-spacings and intensities for the η-phase, which they were unable to index decisively.

The δ-phase of the Np–U system is isomorphous with the ζ-phase of Pu–U (Mardon & Pearce, 1959). This phase is also characterized by a very wide homogeneity range and by deviations from apparent cubic symmetry at high temperatures.

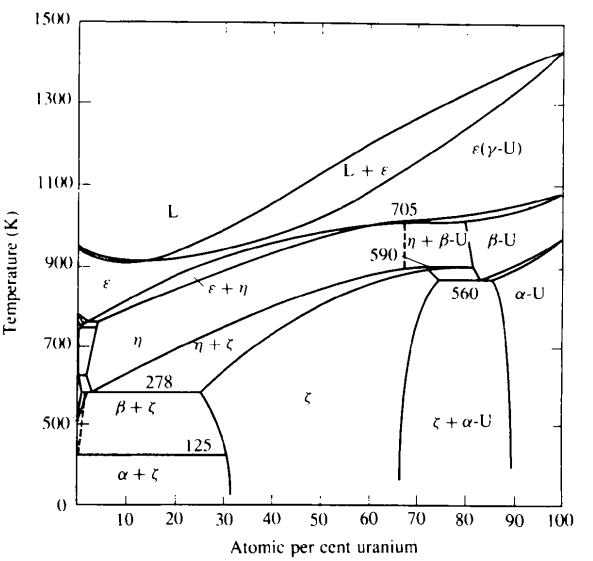

Fig. 1. Phase diagram of the Pu–U system.

2. Experimental

The sample of $Pu_{0.60}U_{0.40}$ was prepared from depleted U and ^{242}Pu of 95% isotopic purity. Appropriate quantities were melted together six times by arc-melting. The ingot was then extruded at 723 K using an 8 mm diameter dye under 54 MPa (8000 p.s.i.) pressure. A cylinder of approximate dimensions 6 (diameter) × 25 mm (length) was machined from the ingot and used for the diffraction experiment. In subsequent heat treatments, the ingot was heated to 623 K for 1 d, furnace-cooled again to room temperature, heated to 873 K for an additional day and furnace-cooled again to room temperature.

The material is radioactive and had to be contained for radiological purposes. Vanadium is an ideal choice for the containment material as it has a very small coherent neutron scattering cross section and favorable mechanical and chemical properties over the anticipated range of temperatures of the experiment. We verified the chemical compatibility of the materials by holding a small sample of $Pu_{0.60}U_{0.40}$ in contact with vanadium at 873 K in an argon atmosphere for 72 h. To achieve radiological containment, the cylindrical diffraction sample was placed in a loosely fitting thin-walled vanadium tube. The tube was sealed in an argon–helium atmosphere by insertion of a cap that was initially held at liquid nitrogen temperature and sealed by expansion upon warming to room temperature; an additional seal was made by heli-arc welding. This sealed assembly was then sealed again by the same method into a larger vanadium tube, so that the sample was doubly contained.

Diffraction experiments were conducted on the general purpose powder diffractometer (GPPD) at the Intense Pulsed Neutron Source (IPNS) at Argonne National Laboratory.* Data were collected at each of eight temperatures between 302 and 818 K. We used a furnace designed by Vaninetti and Lawson that was designed for very precise temperature control and carefully controlled heating rates (Mueller, Richardson, Strain & Hofman, 1991). Data from the ±148, ±90 and ±60° detector banks in the range $0.6 \le d < 5.3$ Å were analyzed and co-refined with the Rietveld package contained in the General Structural Analysis Program (GSAS) (Larson & Von Dreele, 1986).

3. Results

In agreement with the phase diagram, the five data sets with temperatures at or below 673 K showed a single-phase–ζ-phase pattern. Fig. 2 shows some of the data from our neutron diffraction experiment. These data are from the high-angle (±148°) detector banks of GPPD with the sample near room temperature. (Because of self-heating, the measured sample temperature was 302 K.) The data have been fit by Rietveld refinement using a model to be discussed later. Fig. 3 shows the detail of the diffraction pattern.

In agreement with Ellinger, Elliott & Cramer (1959), we found that the metric symmetry of the ζ-phase is pseudocubic. We used the cubic cell as the starting point of a series of Le Bail refinements that eventually fit the data with a rhombohedral unit cell, with lattice constants a = 10.6853 Å, α = 89.736°.

We used the space group $R3$ in the next stage of structural refinement. To obtain a plausible starting structure, we picked the atomic positions corresponding to those of α-Mn. This choice was made for structural reasons other than the status of α-Mn as a self-intermetallic compound. α-Mn is cubic, $I\bar{4}3m$, also with 58 atoms per unit cell observed for the ζ-phase. Set in the subgroup $R3$, the α-Mn structure has 22 atoms in the asymmetric unit. The initial fits to the data were exceedingly poor, indicating a strong dissimilarity between the structures of α-Mn and the ζ-phase. However, as the refinement proceeded, the actual symmetry of the ζ-phase began to

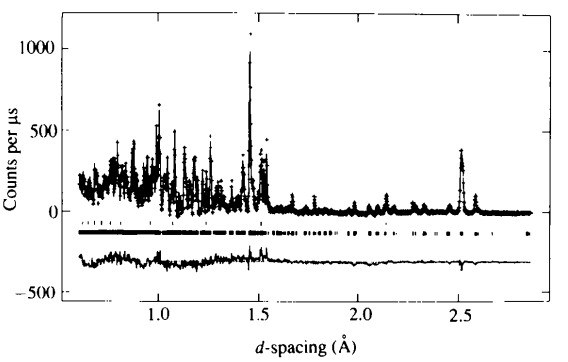

Fig. 2. Diffraction pattern of the ζ-phase $Pu_{0.60}U_{0.40}$ for $0.6 < d < 3.0$ Å. The crosses are the observed intensities and the line is the Rietveld fit. The small vertical ticks indicate the positions of the allowed *hkl* reflections. The lower row of ticks is for the ζ-phase and the upper row is for the vanadium containment. The difference between the observed and calculated profiles is plotted below the diffraction pattern.

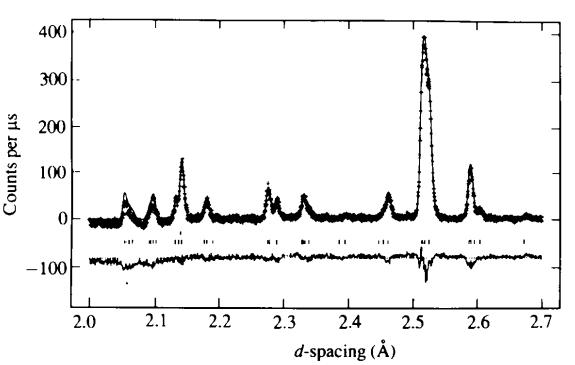

Fig. 3. Diffraction pattern of the ζ-phase $Pu_{0.60}U_{0.40}$ for $2.0 < d < 2.7$ Å. See the caption of Fig. 2 for details.

* The numbered intensity of each measured point in the profile has been deposited with the IUCr (Reference: VS0125). Copies may be obtained through The Managing Editor, International Union of crystallography, 5 Abbey Square, Chester CH1 2HU, England.

reveal itself in relationships between the refined values of the atomic positions. We progressively increased the symmetry (and decreased the number of atoms) until the final structure was reached. At one point, during an intermediate stage with $R3m$, the refinement stalled with unacceptably short bond lengths for one of the atoms. A better position for the offending atom was chosen by inspection of diagrams of the intermediate structure and the subsequent refinements proceeded smoothly.

The refined structure has space group $R\bar{3}m$ with ten atoms in the asymmetric unit. Because of the close similarity of the scattering lengths for ^{242}Pu and U (0.81 and 0.83 $\times$ 10^{-12} cm, respectively), we were unable to investigate the possibility of atomic ordering in the structure. The atoms are referred to simply as Pu. We used a single isotropic thermal factor for all the atoms. The atomic positions are given in the rhombohedral setting in Table 1 and in the hexagonal setting in Table 2. For the data taken at 302 K, we obtained satisfactory agreement factors: a weighted profile R of 3.84% with a reduced χ^2 of 2.73 for 46 variables. For the higher temperature data, the R's are somewhat higher and the χ^2's somewhat lower because of reduced counting times. Three views of the structure are shown in Figs. 4, 5 and 6. Note that the (111)- and (11$\bar{1}$)-projections are quite different. Bonds with lengths < 3.00 Å are shown as an aid to the interpretation of the structure. The observed bond lengths are quite reasonable, as shown in the histograms of Fig. 7.

At higher temperatures, we also obtained data on the η-phase. We observed a complex diffraction pattern that contains fewer long d-spacing reflections than observed

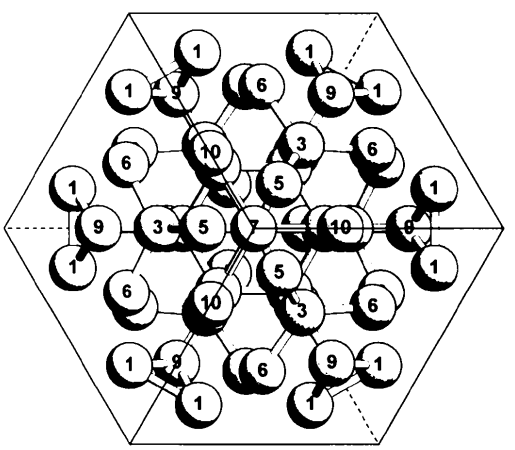

Fig. 4. Structure of the ζ-phase $Pu_{0.60}U_{0.40}$, (111)-projection. Bonds of length < 3.00 Å are shown.

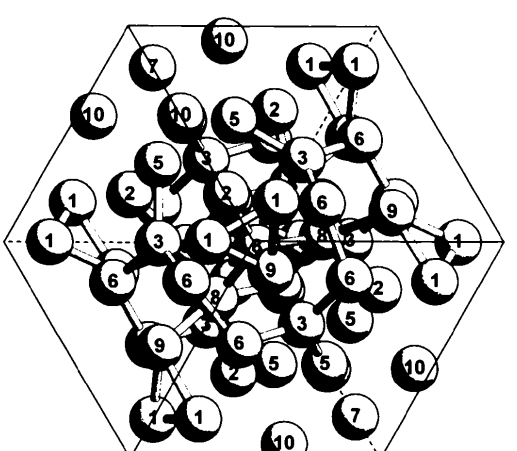

Fig. 5. Structure of the ζ-phase $Pu_{0.60}U_{0.40}$, (11$\bar{1}$)-projection. Bonds of length < 3.00 Å are shown.

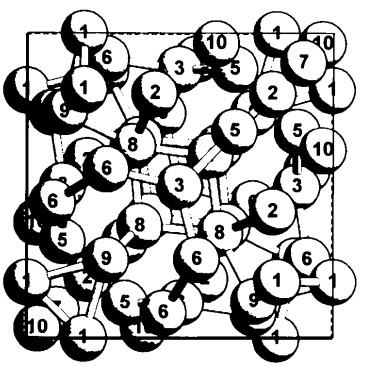

Fig. 6. Structure of the ζ-phase $Pu_{0.60}U_{0.40}$, (100)-projection. Bonds of length < 3.00 Å are shown.

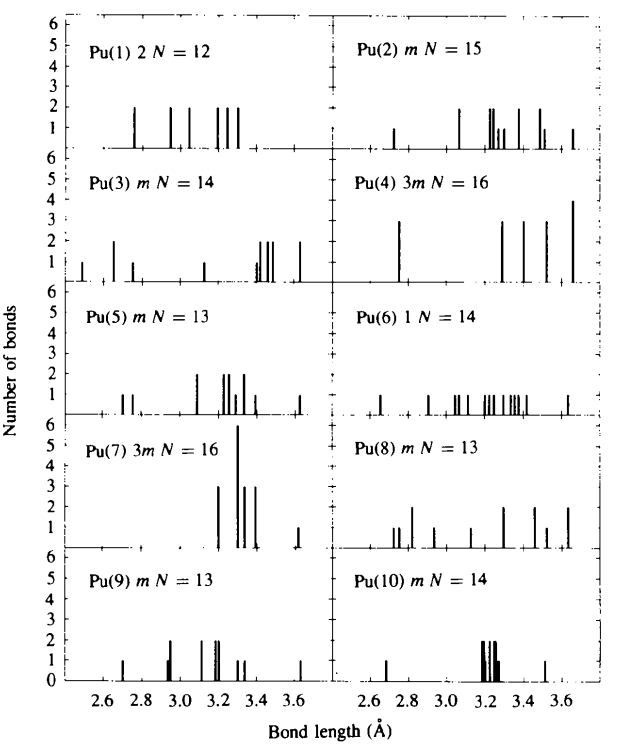

Fig. 7. Number of bonds *versus* bond length for each of the 10 atoms of the ζ-phase $Pu_{0.60}U_{0.40}$ at 302 K. Each panel shows the atom identifier, the site symmetry and the total number of bonds with length < 3.70 Å. See Table 4.

Table 1. *Fractional atomic coordinates and site symmetry for ζ-phase $Pu_{0.6}U_{0.4}$ (rhombohedral setting)*

	x	*y*	*z*	Site symmetry
Pu1	0.8171 (3)	0.1829 (3)	0.0	2
Pu2	0.5852 (4)	0.1964 (2)	0.1964 (2)	*m*
Pu3	0.5028 (2)	0.5028 (2)	0.1167 (3)	*m*
Pu4	0.4018 (3)	0.4018 (3)	0.4018 (3)	3*m*
Pu5	0.3212 (2)	0.3212 (2)	0.1159 (3)	*m*
Pu6	0.7424 (2)	0.4454 (2)	0.0820 (3)	1
Pu7	0.0974 (3)	0.0974 (3)	0.0974 (3)	3*m*
Pu8	0.6309 (3)	0.6309 (3)	0.3447 (3)	*m*
Pu9	0.7427 (2)	0.7427 (2)	0.1194 (4)	*m*
Pu10	0.3838 (3)	0.0348 (2)	0.0348 (2)	*m*

Table 2. *Fractional atomic coordinates and site symmetry for ζ-phase $Pu_{0.6}U_{0.4}$ (hexagonal setting)*

	x	*y*	*z*	Site symmetry
Pu1	0.1829 (3)	0.1829 (3)	0.0	2
Pu2	0.4075 (3)	0.2037 (1)	0.0073 (2)	*m*
Pu3	0.4621 (14)	0.5379 (1)	0.0408 (2)	*m*
Pu4	1/3	2/3	0.0685 (3)	3*m*
Pu5	0.5982 (1)	0.4018 (1)	0.0805 (2)	*m*
Pu6	0.3555 (2)	0.3476 (2)	0.0899 (1)	1
Pu7	0.0	0.0	0.0974 (3)	3*m*
Pu8	0.2379 (1)	0.4758 (3)	0.1312 (2)	*m*
Pu9	0.1256 (2)	0.2512 (3)	0.1318 (2)	*m*
Pu10	0.2326 (3)	0.11632(1)	0.1511 (2)	*m*

by Ellinger, Elliott & Cramer (1959). However, we have not arrived at a satisfactory indexing of the pattern and discussion of these data must be postponed.

Fig. 8 shows the lattice constants of $Pu_{0.60}U_{0.40}$ plotted *versus* temperature. We have fitted parabolas to a and α, but these fits do not have any physical significance. The rhombohedral angle α has an intriguing temperature dependence: it is close to 90° near room temperatures, but decreases rapidly with increasing temperature. This behavior of α explains the pseudocubic appearance of the diffraction patterns. It has so far not been possible to extend this study to lower temperatures.

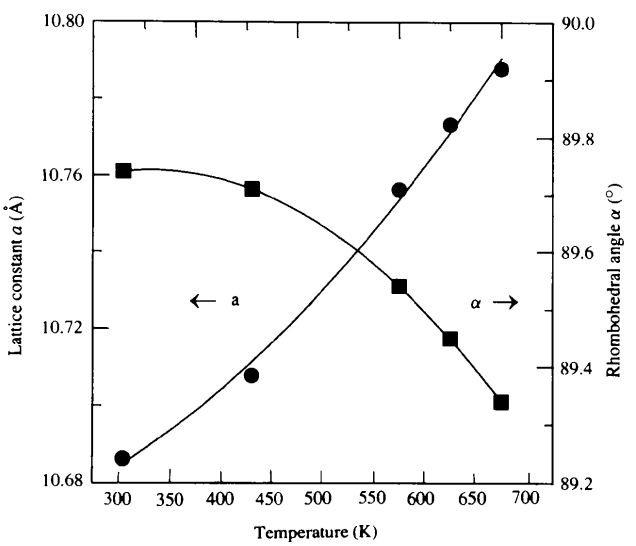

Fig. 8. Lattice constants of the ζ-phase $Pu_{0.60}U_{0.40}$ *versus* temperature. The error bars are smaller than the plotted points. There is no physical significance to the fitted lines.

Fig. 9 shows the temperature dependence of the average mean square thermal displacement obtained from the refined thermal factors. We have fitted (Lawson *et al.*, 1991) these data to a simple Debye model and obtained a Debye–Waller temperature, $\theta_{DW} = 118\,(2)$ K, which characterizes the elastic behavior of the ζ-phase.

4. Discussion

The structural complexity of the ζ-phase is typical of actinide systems. Pure Pu metal has a complicated sequence of structures as the temperature is increased and the structure becomes simple only for the high temperature δ- and ε-phases. Complex structures are also found for many Pu intermetallics. Table 3 shows a representative collection of these structures. Such a table is necessarily incomplete, because many of the complex Pu alloy structures have not been solved, most notably Pu_4Zr, Pu_3Th and the η-phase of the Pu–U and Pu–Np systems. All the structures of Pu metal are included. The structure of α-Mn is also included for reference.

The structure of the ζ-phase $Pu_{0.60}U_{0.40}$ is similar to that of α-Mn in that 58 atoms are contained in an approximately cubic unit cell. The space group of the ζ-phase ($R\bar{3}m$) is a subgroup of that of α-Mn ($I\bar{4}3m$). However, the structures are not at all the same. Figs. 10 and 11 show two views of the α-Mn structure. Fig 10 should be compared with Figs. 4 and 5, and Fig. 11 should be compared with Fig. 6. Fig. 10 shows both the (111)- and (11$\bar{1}$)-projections; these are the same for the cubic structure of α-Mn.

As with α-Pu, the ζ-phase has many short bonds. The shortest bond length, at 2.488 Å, is similar to that

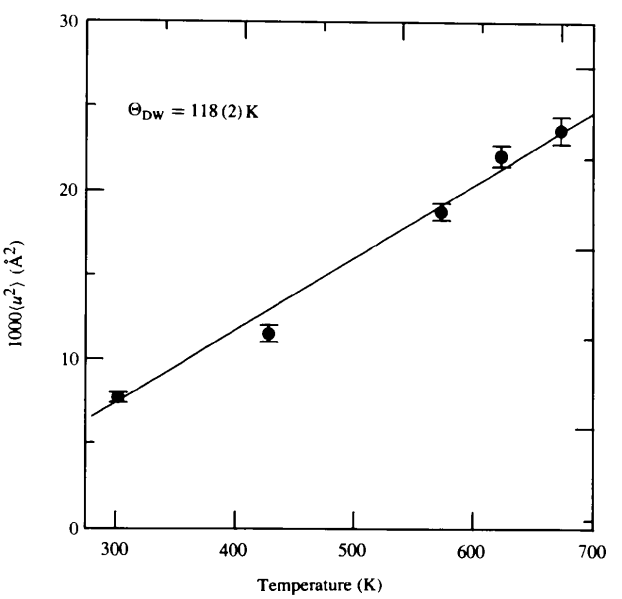

Fig. 9. Average isotropic mean-square atomic thermal displacements of the ζ-phase $Pu_{0.60}U_{0.40}$ *versus* temperature. The line is a fit to a simple Debye model.

Table 3. *Structures of ζ-$Pu_{0.60}U_{0.40}$ and related phases*

Phase	Space group	Atom types	Pearson symbol	Refs.
α-U	*Cmcm*	2	oC4	(*a*)
β-U	$P4_2/mnm$	6	tP30	(*a*,*b*)
γ-U	*Im3m*	1	cI2	(*a*)
α-Pu	$P2_1/m$	8	mP16	(*a*,*c*)
β-Pu	*I2/m*	7	mC34	(*a*,*d*)
γ-Pu	*Fddd*	1	oF8	(*a*)
δ-Pu	*Fm3m*	1	cF4	(*a*)
δ'-Pu	*I4/mmm*	1	tI2	(*a*)
ε-Pu	*Im3m*	1	cI2	(*a*)
ζ-$Pu_{19}Os$	*Pnna*	8	oP52	(*e*)
ζ-$Pu_{28}Zr$	$I4_1/a$	8	tI116	(*f*)
α-Mn	$I\bar{4}3m$	4	cI58	(*a*,*g*)
ζ-phase	$R\bar{3}m$	10	hR58	(*h*)

References: (*a*) Donohue (1974); (*b*) Lawson, Olsen, Richardson, Mueller & Lander (1988); (*c*) Zachariasen & Ellinger (1963*b*); (*d*) Zachariasen & Ellinger (1963*a*); (*e*) Cromer (1979*a*); (*f*) Cromer (1979*b*); (*g*) Bradley & Thewlis (1927); (*h*) this study.

Table 4. *Short bonds (<3.00 Å) in ζ-$Pu_{0.60}U_{0.40}$*

Atom	Site symmetry	Multiplicity	Number of bonds (<3.70 Å)	Number of short bonds (<3.00 Å)	Average short bond length
1	2	6	12	4	2.85 (13)
2	*m*	6	15	1	2.73
3	*m*	6	14	4	2.64 (11)
4	3*m*	2	16	3	2.75
5	*m*	6	13	2	2.73 (4)
6	1	12	14	2	2.78 (18)
7	3*m*	2	16	0	—
8	*m*	6	13	5	2.81 (8)
9	*m*	6	13	4	2.88 (12)
10	*m*	6	14	1	2.69

observed for α-Pu. The distribution of short bonds in the ζ-phase is shown in Table 4. Long and short bonds are not as well separated in the ζ-phase as in α-Pu, so we have arbitrarily set the maximum distance for short bonds at 3.0 Å. The average short bond lengths are also shown, together with the standard deviations of this average. This average is obviously biased by the arbitrary choice of maximum distance. For reference, the bond length for δ-Pu is 3.28 Å. The existence of these short bonds suggests that the structural complexity is due to the tendency of Pu to maximize bonding by 5*f* electrons. This tendency also shows up in the band structure calculations for α-Pu metal (van Ek, Sterne & Gonis, 1993).

It does not appear to be possible to identify the atoms on the basis of observed bond lengths. Such an assignment would be desirable to account for alloy composition and homogeneity range. This question would be better studied in the δ-phase of the Np–U system, where there is a favorable contrast in the nuclear scattering lengths. Anomalous X-ray diffraction could also be used to advantage in either alloy system.

Fig. 12 shows the average atomic volume of the ζ-phase plotted *versus* temperature, together with those of other light actinides (Lawson, Goldstone, Cort, Sheldon & Foltyn, 1994*b*). The atomic volume of ζ-phase is close to that of α-U, so that the average atomic volume for Pu in the ζ-phase is 21.17 Å^3, only a little higher than that of α-U. Following the assignments made by Zachariasen (1973), this implies an atomic radius for Pu of 1.553 Å, a value that is intermediate between that of α-Pu and β-Pu. It is possible that more than one Pu configuration is present in the ζ-phase. The average linear thermal expansion of the ζ-phase is almost as high as that of α-Pu.

Table 5 shows the Debye–Waller temperature, θ_{DW}, of the ζ-phase determined from the data of Fig. 9. The table includes the Debye–Waller temperatures of the other light actinide phases that have been determined so far (Lawson, Goldstone, Cort, Sheldon & Foltyn, 1994*a*,*b*). The ζ-phase has the lowest θ_{DW}; however, the θ_{DW}'s of the other phases decrease rather strongly with increasing temperature, reflecting a general weakening of the bonding. Therefore, one must be careful about specifying the temperature at which comparisons are made.

5. Summary and concluding remarks

We have solved the structure of the ζ-phase of the Pu–U system. It is a complicated structure, space group

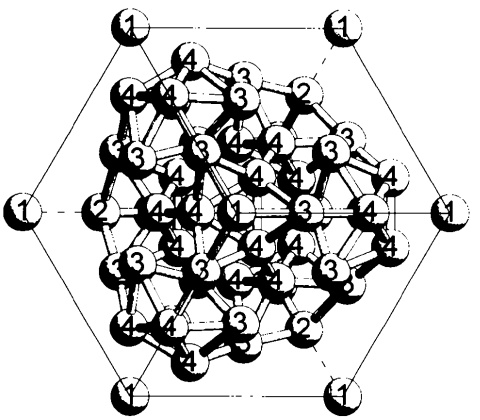

Fig. 10. Structure of α-Mn, (111)-projection. Bonds of length < 2.60 Å are shown.

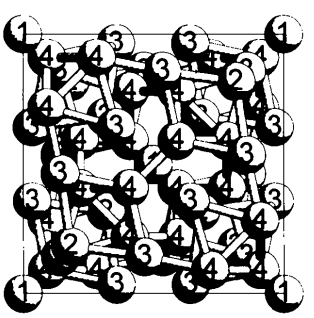

Fig. 11. Structure of α-Mn, (100)-projection. Bonds of length < 2.60 Å are shown.

$R\bar{3}m$, with 58 atoms in the primitive unit cell and ten atoms in the asymmetric unit. As with α-Pu, the structure is characterized by the occurrence of short bonds. Although we were unable to study the question of atomic ordering in this phase, this problem could be attacked by other means. We determined the variations of the lattice constants and thermal factors with temperature and we extracted thermal expansion and Debye–Waller parameters.

The general features of the structure – complexity together with short bonds – fit the overall pattern for the light actinides. Independent of the question of ordering in the ζ-phase, it is clear that the structure is that of a very complicated self-intermetallic compound. It is by the formation of such compounds that the maximum 5*f* bonding can be achieved.

This work was supported under the auspices of the United States Department of Energy. The Intense Pulsed Neutron Source is operated as a National User Facility by the United States Department of Energy Basic Energy Sciences – Materials Sciences, under contract No. W-31-109-ENG-38. The crystallographic diagrams used in this research were prepared using the program *Atoms*. We wish to thank Dennis Wozniak of IPNS, Janice Aasen, Felix Chavez and Patricia Wright of LANL, and members of the Radiation Protection Staff at Argonne National Laboratory for their essential assistance with the experiment. We are grateful to David Eash of LANL for advice on sample preparation, to George Kwei, Kimberly Martin, Michael Stevens, Robert Sheldon and Karl Staudhammer for comments on the manuscript, and especially to Reed Elliot for the discussions which led to this experiment.

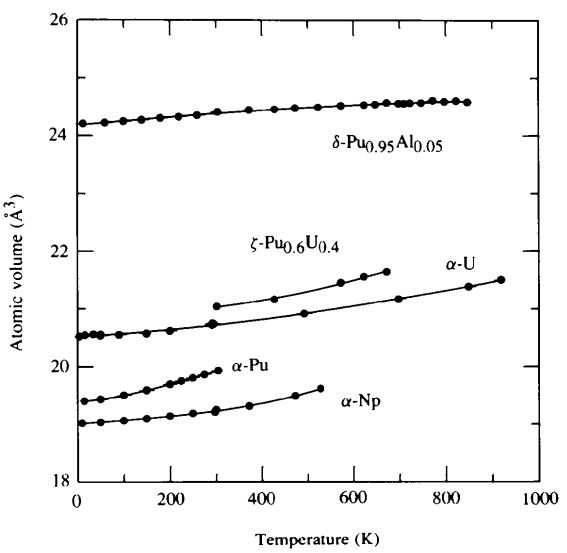

Fig. 12. Actinide volume *versus* temperature of the ζ-phase $Pu_{0.60}U_{0.40}$ and light actinide elements and some Pu alloys.

Table 5. *Debye–Waller temperatures of the light actinide metals*

Phase	Θ_{DW} (K)
α-U	260 (4)
α-Np	269 (10)
α-Pu	201 (5)
δ-Pu	132 (1)
ζ-$Pu_{0.60}U_{0.40}$	118 (2)

References

Bradley, A. J. & Thewlis, J. (1927). *Proc. R. Soc. A*, **115**, 456–471.

Cromer, D. T. (1979*a*). *Acta Cryst.* B**35**, 14–19.

Cromer, D. T. (1979*b*). *Acta Cryst.* B**35**, 1945–1949.

Donohue, J. (1974). *The Structures of the Elements*, pp. 128–167. New York: John Wiley and Sons.

Ek, J. van, Sterne, P. A. & Gonis, A. (1993). *Phys. Rev. B*, **48**, 16280–16289.

Ellinger, F. H., Elliott, R. O. & Cramer, E. M. (1959). *J. Nucl. Mater.* **1**, 233–243.

Grigorvich, V. K. (1988). *The Metallic Bond and the Structure of Metals*, pp. 172–177. Commack, New York: Nova Science Publishers.

Larson, A. C. & Von Dreele, R. B. (1986). Report LAUR 86-748. General Structure Analysis System, Los Alamos National Laboratory, Los Alamos, New Mexico, USA.

Lawson, A. C., Goldstone, J. A., Cort, B., Sheldon, R. I. & Foltyn, E. M. (1994*a*). *Actinide Processing: Methods and Materials*, edited by B. Mishra & W. A. Averill, pp. 31–44. Warrendale, Pennsylvania: TMS.

Lawson, A. C., Goldstone, J. A., Cort, B., Sheldon, R. I. & Foltyn, E. M. (1994*b*). *J. Alloys Compd.* **213/214**, 426–428.

Lawson, A. C., Olsen, C. E., Richardson, J. W. Jr, Mueller, M. H. & Lander, G. H. (1988). *Acta Cryst.* B**44**, 89–96.

Lawson, A. C., Williams, A., Goldstone, J. A., Eash, D. T., Martinez, R. J., Archuleta, J. I., Martinez, D. J., Cort, B. & Stevens, M. F. (1991). *J. Less-Common Met.* **167**, 353–363.

Mardon, P. G. & Pearce, J. H. (1959). *J. Less-Common Met.* **1**, 467–475.

Mueller, M. H., Richardson, J. W. Jr, Strain, R. V. & Hofman, G. L. (1991). *Advances in X-Ray Analysis*, edited by C. S. Barett, J. V. Gilfrich, J. C. Noyen, T. C. Huang & P. K. Predecki, Vol. 34, pp. 447–457. New York: Plenum Press.

Okamoto, Y., Maeda, A., Suzuki, Y. & Ohmichi, T. (1994). *J. Alloys Compd.* **213/214**, 372–374.

Zachariasen, W. H. (1973). *J. Inorg. Nucl. Chem.* **35**, 3487–3497.

Zachariasen, W. H. & Ellinger, F. H. (1963*a*). *Acta Cryst.* **16**, 369–375.

Zachariasen, W. H. & Ellinger, F. H. (1963*b*). *Acta Cryst.* **16**, 777–783.